FINAL REPORT

AN INVESTIGATION OF THE LOSS OF DUCTILITY IN HYDROGEN CHARGED β–Ti ALLOYS

NASA Grant No. NAG 2-852

Submitted by. Prof. I. M. Robertson
Dept. of Materials Science and Engineering
University of Illinois

The high strength, low density, and good corrosion resistance of Ti-based alloys make them candidate materials for a number of applications in the aerospace industry. A major limitation in the use of these alloys in the advanced hypersonic flight vehicle program is their susceptibility to hydrogen embrittlement. This study focuses on the hydrogen sensitivity of TIMETAL 21S beta-Ti alloy. The material received was in the form of grip-ends of failed tensile test samples which had been exposed to different charging conditions (combinations of hydrogen pressure and temperature). The samples received, the charging conditions and their fracture mode are listed in Table 1. From Table 1 it can be seen that the fracture behavior changes from ducyile to brittle with increasing hydrogen content, but the transition in behavior occurs for a small increase in hydrogen concentration. The aim of this program was to assess the microstructural differences between the ductile and brittle alloys to ascertain the embrittlement mechanism. To address this problem a range of tools which included x-ray diffraction, scanning electron microscopy (SEM) and transmission electron microscopy (TEM) were used.

In the initial data received from NASA, the hydrogen content of these samples was quoted in arbitrary units; therefore, a first step was to determine the actual hydrogen concentration. The hydrogen content was determined by using a high-temperature extraction gas chromatograph system, the accuracy of the hydrogen concentration determined using this setup is $\pm$ 0.5 at. %. The hydrogen

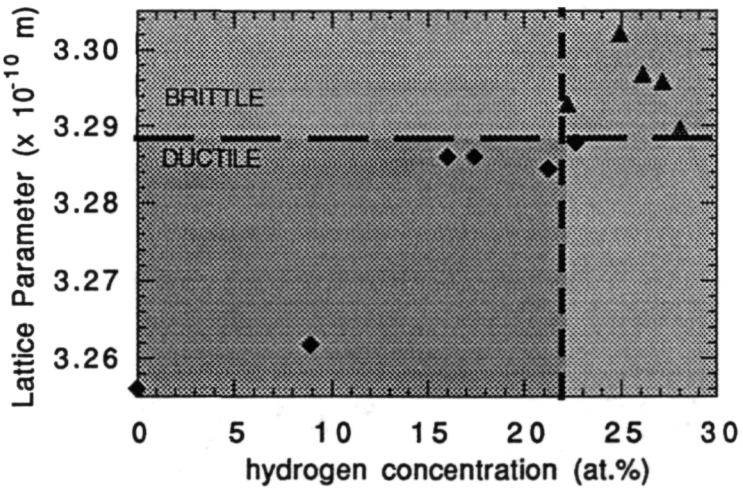

Figure 1. Lattice parameter as a function of hydrogen concentration. ◆ ductile ▲ brittle.

concentrations for the different samples are given in Table 1. Later NASA reports quoted hydrogen concentrations and these are reported in Table 1 for purposes of comparison. The two sets of values are in good agreement.

TABLE 1. Charging conditions, hydrogen concentrations as determined by NASA and at UIUC, lattice parameter of the beta phase, and fracture response for Timetal 21S. Samples charged by NASA unless otherwise stated.

Treatment	Hydrogen Concentration (at%) NASA values	Hydrogen Concentration (at.%)	Lattice Parameter (Å)	Fracture Behavior
1300°F / 40 torr H_2	21	22.2	3.293	brittle
1300°F / 20 torr H_2	17	17.4	3.286	ductile
1200°F / 20 torr H_2	24	24.9	3.302	brittle
1200°F / 10 torr H_2	18	16.0	3.286	ductile
1100°F / 10 torr H_2	28	28.0	3.290	brittle
1100°F / 5 torr H_2	21	22.6	3.288	ductile
1000°F / 5 torr H_2	31	26.1	3.297	brittle
1000°F / 2 torr H_2	23	21.2	3.285	ductile
1290°F/ 20 torr H_2 (UIUC charged)	N. A.	27.1	3.296	brittle
1290°F/ 5 torr H_2 (UIUC charged)	N.A.	8.9	3.262	ductile
as received from McDonnell Douglas (Mill Annealed)	N.A.		3.256	ductile

In addition to determining the hydrogen content of the as-received samples, the lattice parameter of the beta-phase was determined by using x-ray diffraction. To minimize systematic errors, the lattice parameter was determined for a given diffraction peak and plotted as a function of $\cos^2\theta/\sin\theta$, where θ is the Bragg angle. A least squares fit was then made for all diffraction peaks. By extrapolation to $\cos^2\theta/\sin\theta = 0$, the lattice parameter can be determined to an accuracy of $\pm$ 0.001 Å. The values of the lattice parameter for the different samples are presented in Table 1 and in graphical form as a function of hydrogen content in Figure 1. Two lines, a vertical line which indicates the hydrogen concentration (~22 at%) above which the samples fail in a brittle manner and a horizontal line which indicates the lattice parameter above which brittle behavior is expected are drawn on the figure. In trying to determine a critical hydrogen concentration for brittle behavior, a difficulty is encountered for the samples charged at 1100° F/ 5 torr H_2 and at 1300° F/ 40 torr H_2 which have within experimental error the same concentration of hydrogen (22.6 and 22.2 at% H) but exhibit different tensile behavior. The sample charged at 1100° F/ 5 torr H_2 shows a ductile response whereas the sample charged at 1300° F/ 40 torr H_2

shows a brittle response. Assuming that the embrittlement is a consequence of hydrogen in the beta-phase and not in the alpha-phase, this apparent discrepancy can be attributed to microstructural differences. The 1100° F/ 5 torr H_2 (ductile response) sample contains a higher percentage of alpha phase than the 1300° F/ 40 torr H_2 (brittle response) sample; consequently, with more of the hydrogen contained in the alpha phase, the actual hydrogen concentration in the beta phase will be reduced below the critical value. In considering the lattice parameter condition, a horizontal line can be drawn at a beta-phase lattice parameter of 3.289Å which separates the ductile and brittle behavior. As this parameter reflects the concentration of hydrogen in the beta-phase and excludes the alpha-phase, it may be a better parameter for determining a critical concentration of hydrogen to induce the transition.

The relative lattice parameter change due to the absorption of hydrogen, $\Delta a/a$ is plotted as a function of hydrogen concentration in Fig. 2. A least squares fit to this data gives the gradient of the line as 4.65×10^{-4}. Using this value allows conversion from the "critical lattice parameter" for the transition in fracture behavior to a critical hydrogen concentration. For a lattice parameter of 3.289Å, this yields a critical hydrogen concentration of 21.8 at.% , which is in reasonable agreement with the "critical hydrogen concentration" line selected by inspection of Figure 1. The volume change due to hydrogen can also be determined from Fig. 2. The ratio of the volume change per hydrogen atom Δv to the volume of the unit cell Ω is 0.108 giving the volume change per hydrogen atom as 3.7 $Å^3$. The Δv is an indication of the space a H atom will occupy in the BCC lattice; the value obtained here is consistent with values determined for other systems.

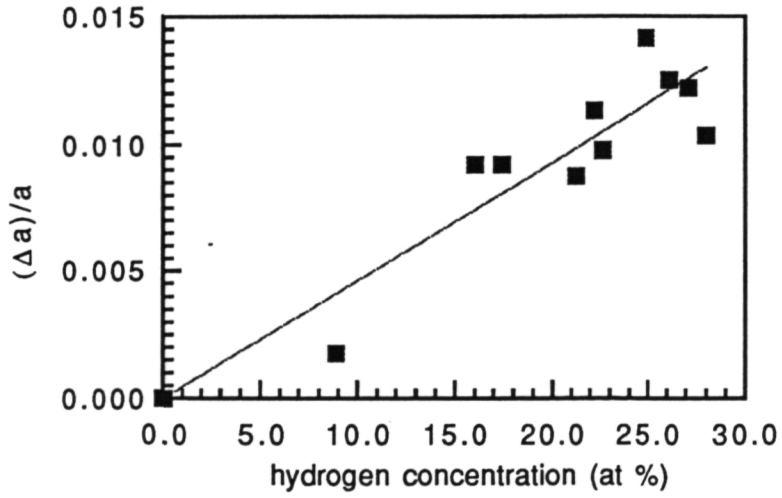

Figure 2. Plot of $\Delta a/a_0$ as a function of hydrogen concentration. a_0 is the lattice parameter of the as-received material

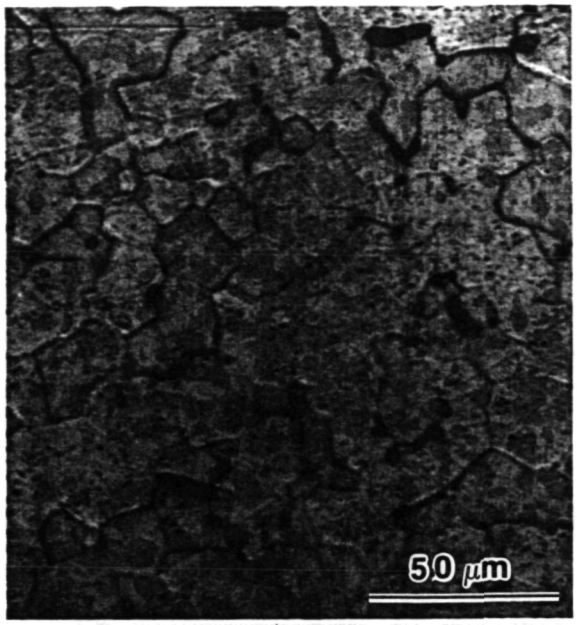

Figure 3. Optical micrograph of an etched as-received sample. The dark regions indicate alpha-phase.

Microstructural Characterization.

In the uncharged state the microstructure of the mill annealed TIMETAL 21S consists predominantly of beta grains with some alpha particles decorating the grain boundaries. An example of this microstructure is shown in the optical micrograph presented in Fig 3; the etchant used reveals the grain boundaries of the beta phase and shows the presence of alpha-phase as the dark-regions on the grain boundaries.

Microstructure of NASA Charged Material

The samples charged at 1300°F (700°C) in 20 and 40 torr of hydrogen gas contained 17 at.% H and 22 at.% H respectively. The sample containing 17 at% H was ductile whereas the other was brittle. TEM examination revealed that the microstructure of both samples consisted primarily of beta grains with a small amount of alpha phase along the grain boundaries; this was consistent with x-ray analysis. Within the beta grains in both samples, rod-shaped precipitates were uniformly dispersed throughout but with a denuded zone near grain boundaries and around large silicide precipitates; an example of these rod-shaped precipitates is shown in Figure 4 for a ductile (4a) and a brittle (4b) sample. Analysis shows that these rods lie along $<001>_{\beta}$ and are about 10 nm in diameter and about 500 nm long. Imaging these rods with different diffraction vectors excited reveals that the strain field associated with these precipitates is radially

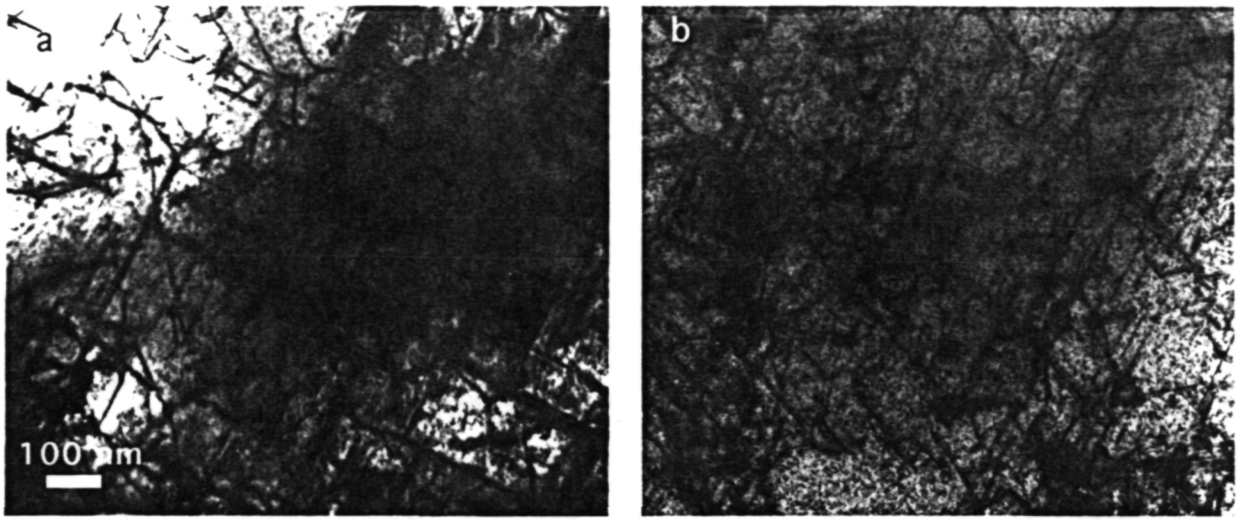

Figure 4. Microstructure formed on charging at 1300°F in (a) 20 and (b) 40 torr of H_2 gas. The beam direction was ~ [001] in (a) and ~ [111] in (b).

Figure 5. Bright-field image formed using g=200 showing that rods with an axis parallel to g show weak contrast.

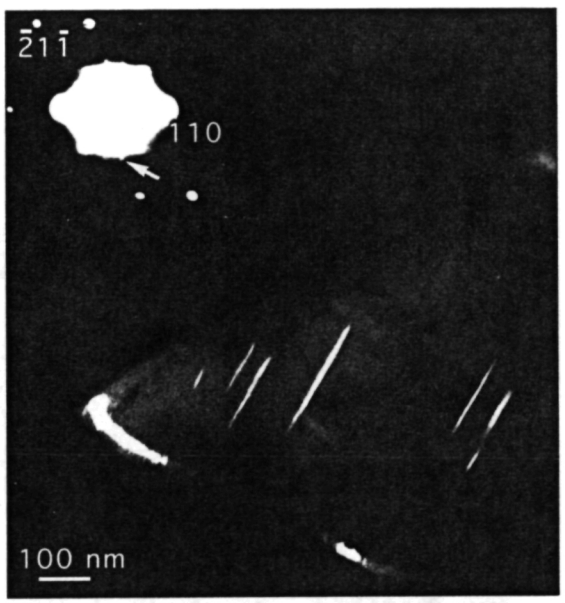

Figure 6. Image of the rod precipitates formed using the extra spot indicated in the diffraction pattern.

symmetric. This is illustrated in Fig. 5 in which the variant of the rods whose line direction is parallel to the diffraction vector is invisible, whereas the variants with rod axis perpendicular to the diffraction condition are visible. Although diffraction spots associated with these rods were identified, insufficient diffraction data was obtained to allow their structure to be determined. Fig. 6 shows a region of sample imaged with the extra spot indicated in the diffraction pattern shown in

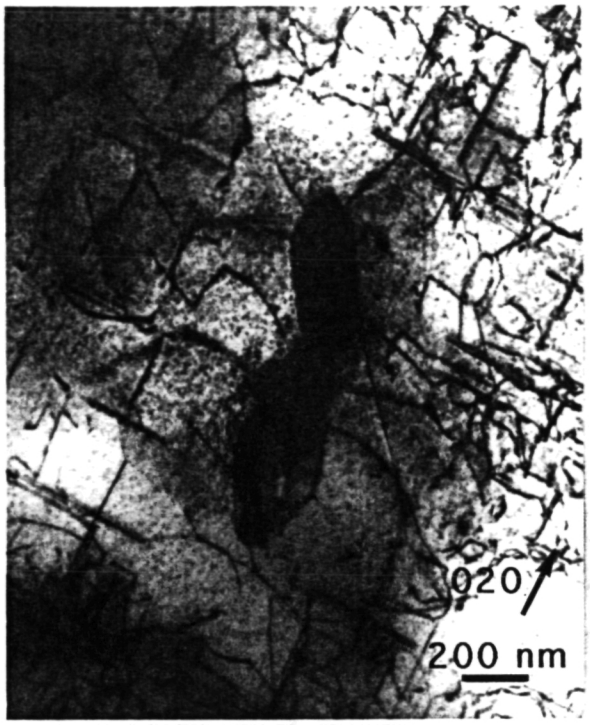

Figure 7. Example of a silicide particle in a beta grain.

the inset. The bright features correspond to the rods observed in the two-beam bright-field images. Larger precipitates also resided within the beta grains, these were identified by energy dispersive spectroscopy as being silicides, Fig 7.

The difficulty in relating the embrittlement to microstructural differences is that samples which contain similar levels of hydrogen and have the same fracture mode have a different microstructure. This problem is highlighted by examining the microstructure of the samples charged at 1100 ^{o}F and comparing them to the samples charged at 1300 ^{o}F. At 1100 ^{o}F samples were exposed to either 10 or 5 torr of hydrogen gas which resulted in hydrogen concentrations of 28 and 22.6 at % H, respectively. The higher hydrogen content sample failed in a brittle manner and the other in a ductile manner. At this charging temperature the microstructures of the brittle and ductile samples were different and in neither case were they similar to the structure observed in the brittle and ductile samples charged at 1300^{o}F. The ductile sample, Fig. 8, consists of mostly beta grains with alpha platelets precipitated along the grain boundaries and within the grains, in agreement with x-ray diffraction studies. Silicide particles were also found distributed throughout the beta grains. This microstructure is consistent with that of an alloy which had experienced a vacuum anneal at a temperature in the range 1200 - 1380 ^{o}F; a larger volume fraction of alpha -phase would be expected in an alloy which had been vacuum annealed at 1100^{o}F. This result is consistent with hydrogen lowering the β-transus temperature.

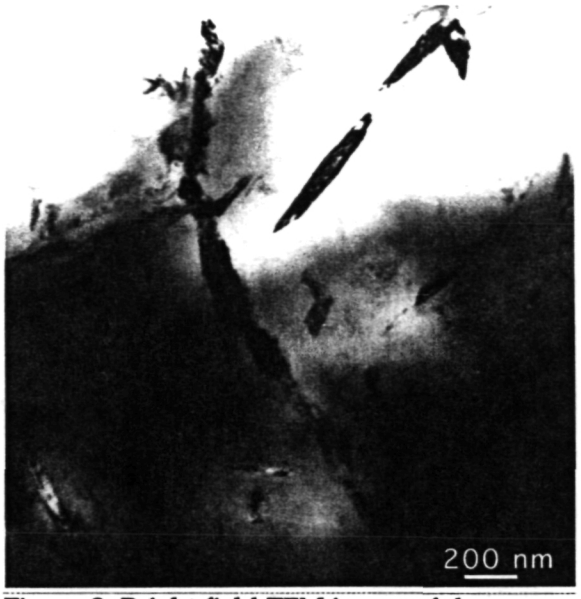

Figure 8 Bright field TEM image of the microstructure in a sample charged in 5 torr of H_2 gas at 1100°F.

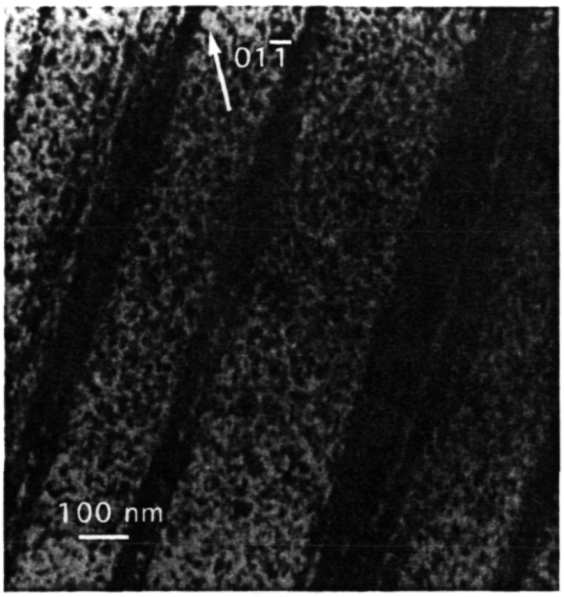

Figure 9. Bright-field TEM image of the microstructure in a sample charged in 10 torr of H_2 gas at 1100°F.

The microstructure in the brittle alloy, Fig 9, was, however, very different from that found in the ductile material. No evidence for any alpha phase was detected by transmission electron microscopy and by X-ray diffraction. Within the beta grains , long, linear defects were present. These defects have a line direction of <111>, and show a change in direction on crossing grain boundaries. The contrast seen within these defects may arise from omega particles. A diffraction contrast analysis of these linear defects demonstrated that, as expected, they exhibit no contrast when imaged with a diffraction vector perpendicular to the line direction. Although this behavior is similar to that of a screw dislocation, these linear features do not display the contrast expected of a line dislocation. No diffraction data could be obtained from these features and their nature is unknown. Another difference between the brittle and ductile materials charged at 1100 °F was the presence of ω-phase in the brittle alloy as evidenced by the streaks in the electron diffraction pattern, Fig. 10. Some evidence for the presence of ω-phase was found in both samples charged at 1300°F.

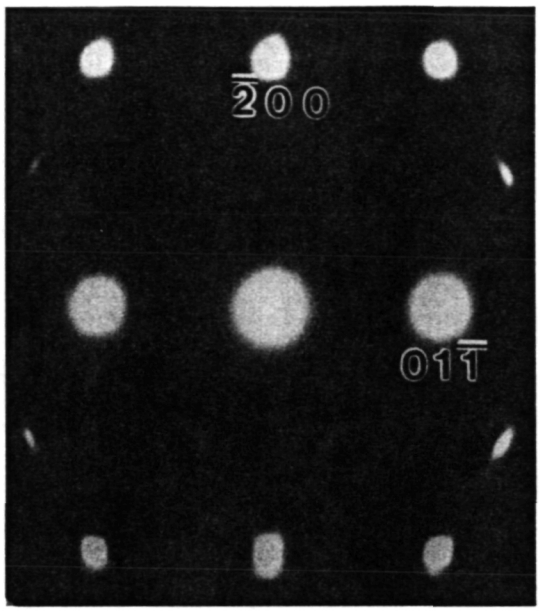

Figure 10. Streaks in the diffraction pattern showing the presence of ω-phase.

1. Surface ground using 400 grit
2. Rinse with methanol
3. Place in hydrogen charging apparatus and evacuate chamber
4. Raise temperature to 1350°F and hold 10 minutes
5. Reduce temperature to charging temperature
6. Charge chamber with high-purity hydrogen
7. Maintain chamber pressure while monitoring hydrogen uptake in specimen
8. *Continue exposure to hydrogen until equilibrium is achieved (no further hydrogen uptake is observed)*
9. Cool in hydrogen environment at a rate of ~150°F min^{-1}*(250°F* min^{-1}) to room temperature.

Fig. 11. Hydrogen charging schedule. (Steps in italics indicate NASA only).

To ensure that the microstructures obtained were not compromised by using the grip-ends of failed tensile samples, new tensile samples and additional coupons from which TEM discs could be made were charged. To permit comparison with the NASA samples, a charging schedule similar to that used by NASA was followed, fig 11. The charging temperature was 1300°F in 20 and in 5 torr of H_2 gas, which resulted in the introduction of 27 at % H and 9 at % H, respectively. The tensile samples were tested in uniaxial tension at room temperature and at a strain rate of 0.05 cm min^{-1}. The sample containing 9 at % H failed in a ductile manner with 18 % elongation, whereas the other sample failed in a brittle manner with 0 % elongation. These results are consistent with the tensile data obtained in the NASA test program. The fracture surfaces of the failed samples were examined by using an SEM and typical fractographs are shown in Fig 12. Figure 12a which is from the ductile sample shows the typical micro-void coalescence failure mechanism. The brittle sample failed transgranularly resulting in a quasi-cleavage fracture surface, 12 b-d. Different features existed on the fracture surface: in some areas small and large steps were found on the large flat fracture surfaces; in other areas features (e.g., dimples and rounding of edges of protrusions) typical of ductile failure were observed; and in yet other areas we observed spalling (e.g. see feature indicated by an arrow in

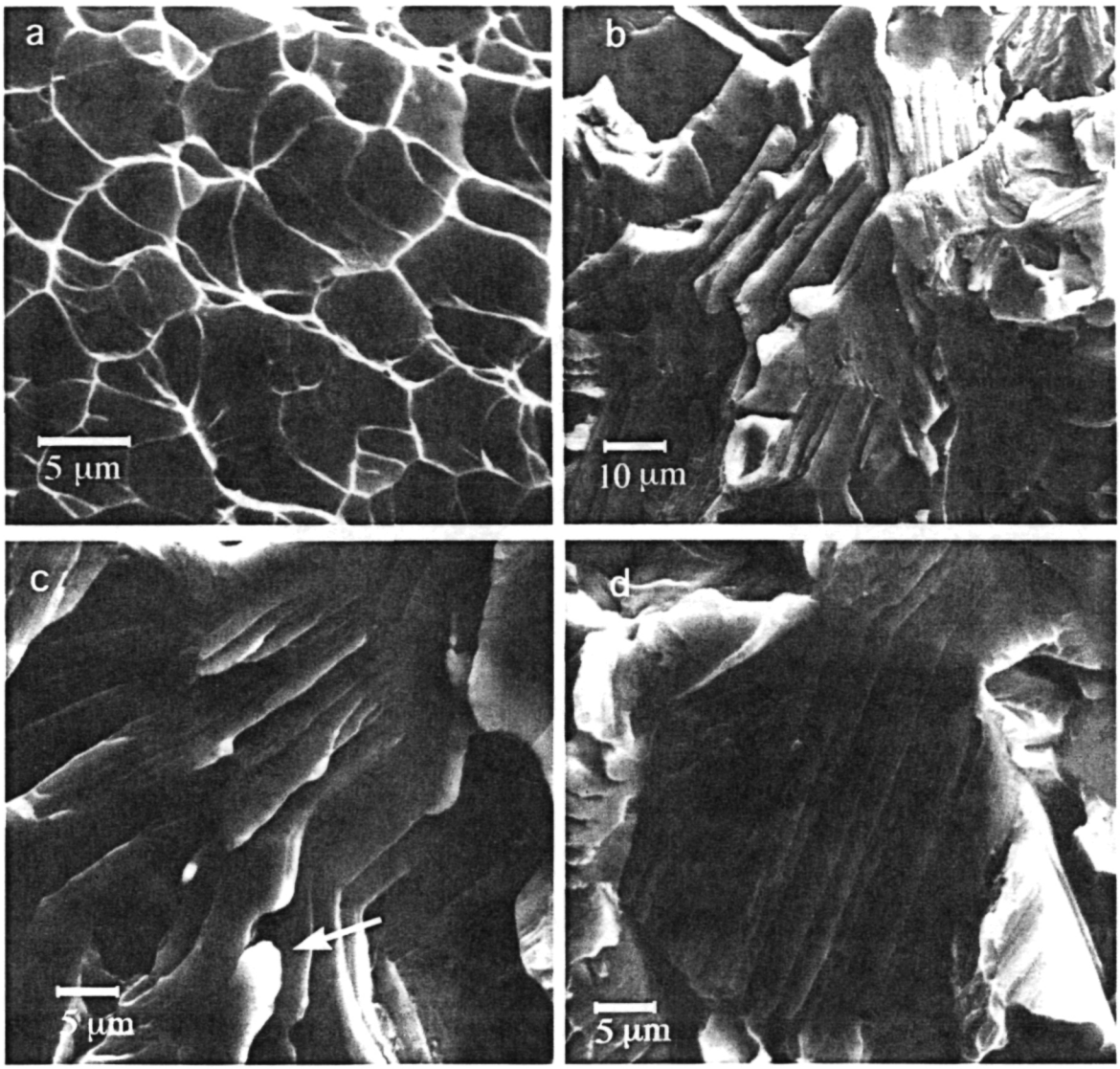

Figure 12. SEM micrographs of the failure surfaces of a sample charged at 1300°F in (a) 5 torr and (b) -(d) 20 torr of H_2 gas.

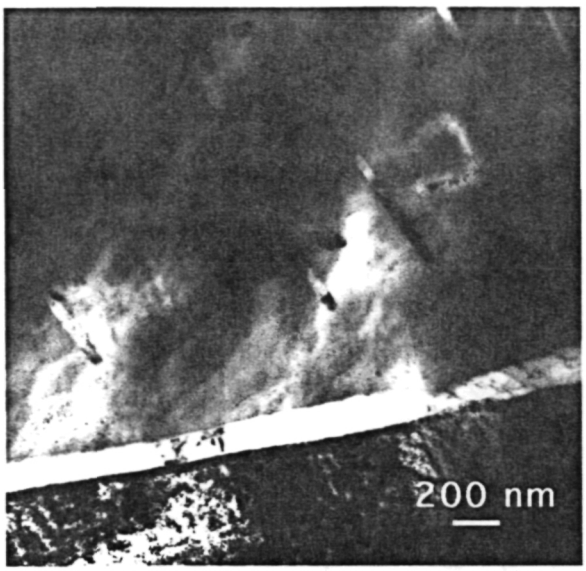

Figure 13. Microstructure in the ductile sample UIUC-charged at 1300°F in 5 torr of H_2 gas.

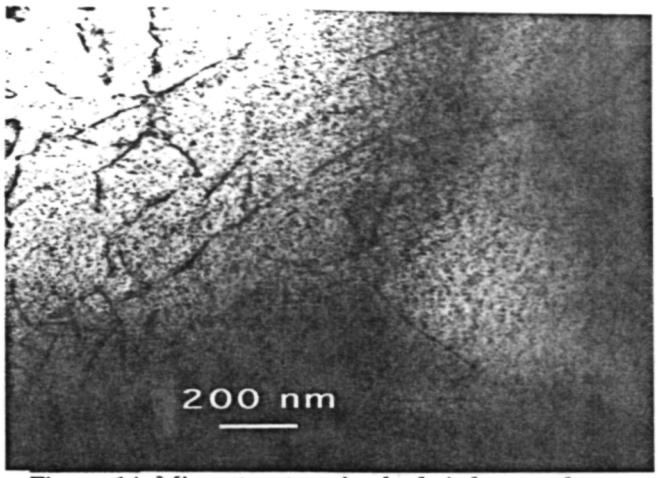

Figure 14. Microstructure in the brittle sample UIUCcharged at 1300°F in 20 torr of hydrogen gas.

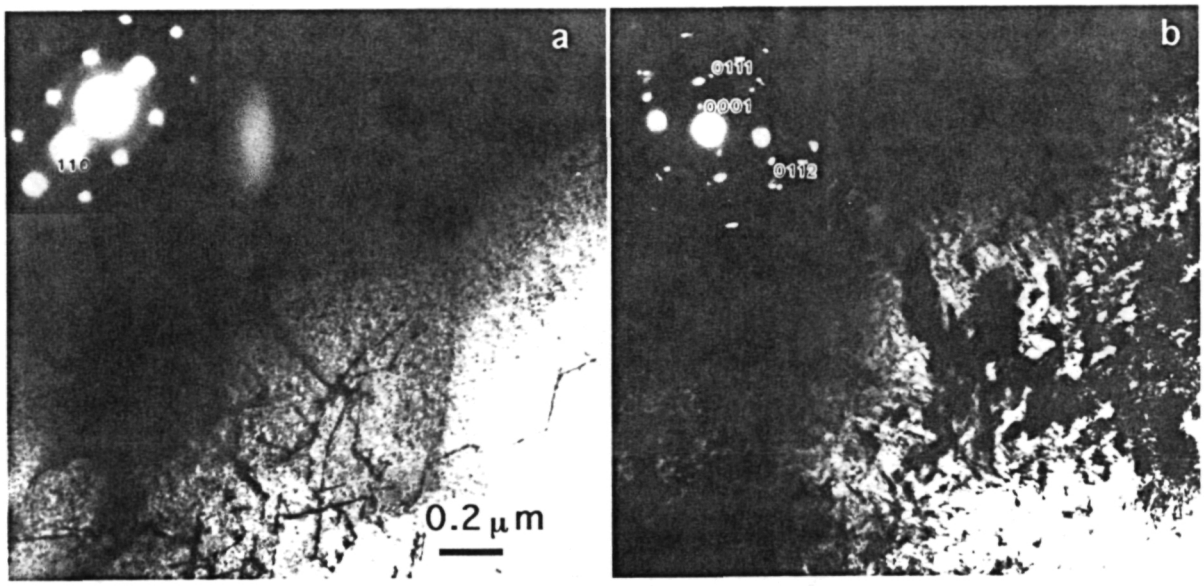

Figure 15. Comparison of the microstructure before (a) and after (b) an anneal at 932°F *in situ* in the TEM.

Fig. 12 c) which might be indicative of the presence of hydrides. A TEM examination of the brittle and ductile samples was performed. The resulting microstructure was again different from the samples charged by NASA at the same charging temperature. The ductile alloy contained a uniform dispersion of alpha particles throughout the beta grains, Fig 13; in the equivalent NASA charged alloy, the ductile sample had small rods distributed throughout the matrix, compare Figs 13 and 4a. The brittle sample contained only beta grains, Fig 14.

To examine the thermal stability of the rod features found in the brittle and ductile samples charged at 1300 °F, samples were annealed *in situ* in the transmission electron microscope. In the sample charged at 1300°F in 20 torr of hydrogen, the strain contrast of the rod-shaped particles began to decrease at a nominal sample temperature of 887 °F. This loss of contrast was not simply a consequence of the foil bending that was occurring during annealing as the sample was tilted to optimize the diffraction contrast of the rods. It was noted that during this annealing procedure the microscope column vacuum increased from $5x10^{-7}$ torr to $8x10^{-7}$ torr. Following an increase in the nominal sample temperature to 932°F, the rods disappeared and were replaced by a very fine Widmanstätten structure which electron diffraction confirmed was due to the precipitation of alpha-phase particles. The dissolution of the rods at 932°F suggests that they may be hydrides or a form of alpha precipitates. The accompanying degradation of the column vacuum may be related to either the outgassing of hydrogen or oxygen from oxide desorption. Again this series of experiments does not unequivocally identify the rods as hydrides.

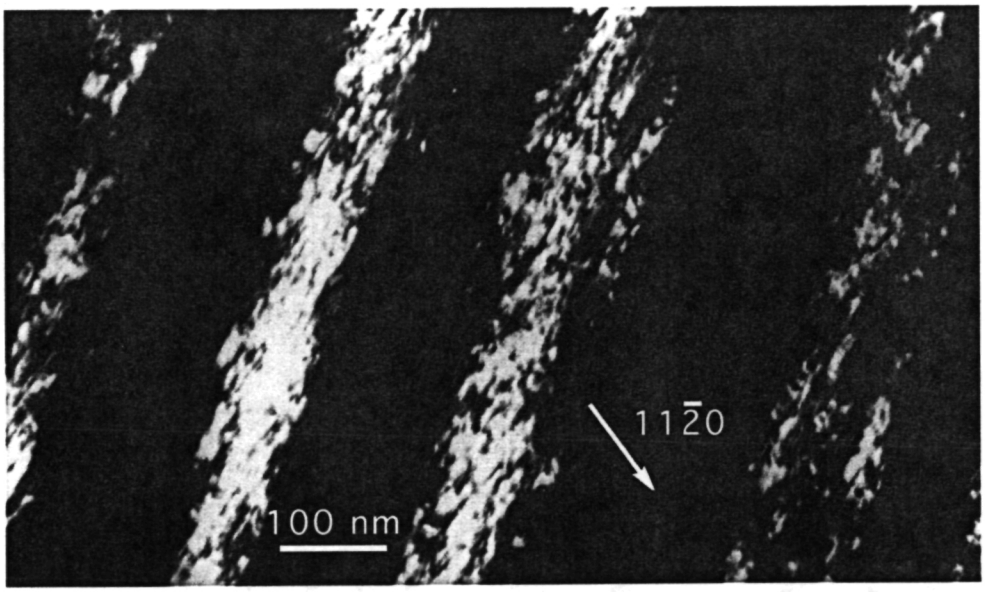

Figure 16. Aligned alpha-needles produced on annealing at 1200°F for 20 minutes *in situ* in the TEM.

An *in situ* annealing experiment was also performed on the brittle sample formed by charging at 1100°F in 10 torr of H_2 gas. Annealing at a nominal sample temperature of 1000°F caused the linear features to broaden. Increasing the sample temperature to 1200°F for 20 minutes, the linear features were replaced by aligned clusters of alpha-needles, see Fig. 16. The long axis of the needles was inclined to the original direction of the linear defect. In addition, small alpha-particles formed throughout the beta matrix.

Annealing in a vacuum furnace at 1100°F for 12 hours at $1x10^{-6}$ torr produced Type 1-alpha (Burgers orientation relationship) and Type 2- alpha (non-Burgers orientation relationship) particles which occupied about 50 % of the beta grains. A continuous layer of alpha-phase now existed along the grain boundaries.

The question therefore remains as to the cause of the loss of ductility in this alloy. Three charging conditions (1300°F/40 torr H_2 (NASA charged), 1100°F/10 torr H_2 (NASA charged) and 1300°F/20 torr H_2 (UIUC charged)) all of which resulted in brittle failure produced three different microstructures. Also in the ductile alloys charged at these different temperatures but in lower pressures of hydrogen gas the alloys exhibited different microstructures. We, therefore, conclude that the production of hydrides in the beta matrix is not responsible for the loss in ductility of these alloys. The mechanisms responsible could not be discerned from this study of the microstructure of charged samples. One possible explanation for the loss of ductility due to internal hydrogen is that hydrides form in the stress field ahead of the advancing crack. To test this hypothesis pre-charged samples were deformed *in situ* in a transmission electron microscope and the region around active cracks examined for the presence of hydrides.

Rectangular (10 x 3 mm) samples for use in the TEM straining stage were made from the ductile and brittle samples charged at 1300 °F. No difference of the crack tip behavior was found between the two samples. Extensive dislocation activity was observed ahead of the propagating cracks in the ductile and brittle material; the cracks eventually propagated along the deformation bands. After allowing the crack to propagate for some distance through the material, the crack was arrested and selected area diffraction patterns were taken from the regions surrounding the crack tip. The diffraction patterns from these regions were complex because of the extent of the deformation and local bending that occurred, but no additional spots which would be consistent with the formation of a hydride was detected. The conclusions from these experiments is that a hydride is not produced in the stress field ahead of the crack. The mechanism responsible for the loss of ductility with a relatively small incremental change in the hydrogen concentration is unknown.

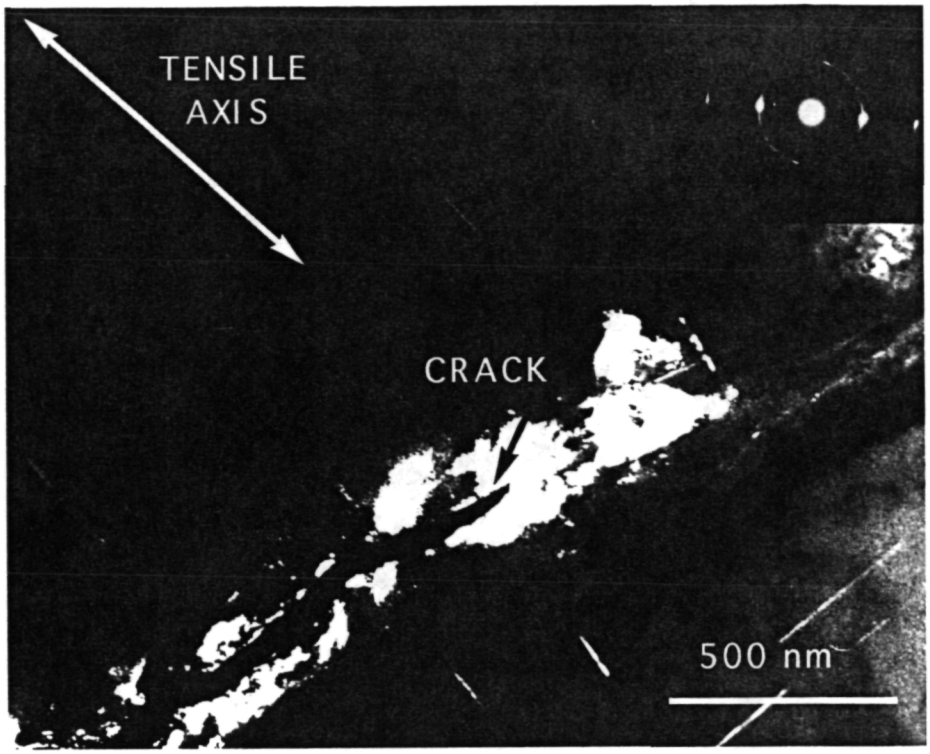

Figure 17. Image of the region around a crack tip. The image was formed using a portion of the ring indicated in the diffraction pattern. The illumination of the rods is due to the coincidental inclusion of a rod diffraction spot.

Hydride formation in TIMETAL-21S

To demonstrate that a hydride can be formed in this alloy and to determine its structure samples were charged at 1290°F for 1 hour in 1 atm H_2 gas and furnace cooled at a rate of 211°F/hr in 1 atm hydrogen gas. This charging condition resulted in a hydrogen concentration of about 59 at.%H. This charging condition resulted in a brittle sample which could be readily powdered. X-ray diffraction analysis of the powdered material showed that it had a FCC structure with a lattice parameter of 4.60 Å, Fig 18. However, the diffraction peaks were rather broad and appeared split at higher angles, which would be consistent with either a tetragonal or orthorhombic structure rather than a face center cubic structure. One calculated structure that fits the x-ray data well is a FCT structure with lattice parameters a = 4.27 Å, c = 4.60 Å and a c/a ratio of 1.078.

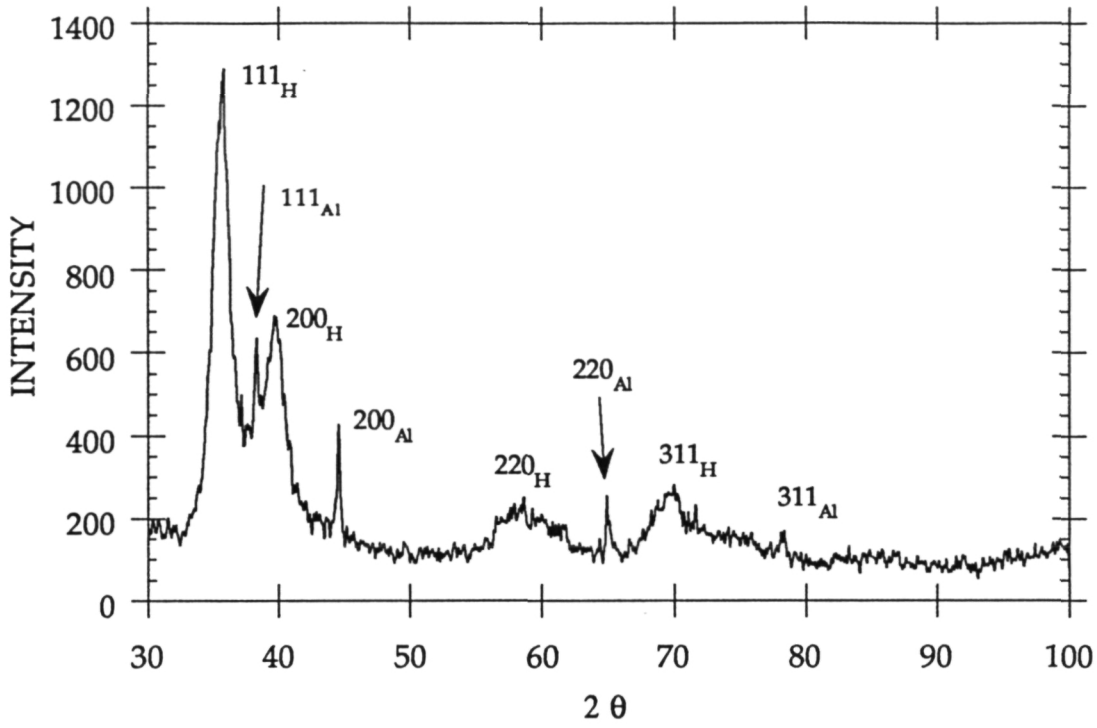

Figure 18. X-ray diffraction scan showing the formation of a hydride in beta-21S. Al peaks due to a sample holder.